Available online at www.sciencedirect.com
SciVerse ScienceDirect
Journal of the European Ceramic Society xxx (2012) xxx–xxx
www.elsevier.com/locate/jeurceramsoc

Influence of the structure of $MgO{\cdot}nAl_2O_3$ spinel lattices on transparent ceramics processing and properties

Andreas Krell *, Katja Waetzig, Jens Klimke

Fraunhofer Institute of Ceramic Technologies and Systems (IKTS), 01277 Dresden, Germany

Abstract

It is demonstrated that a complete elimination of pores on sintering is governed not only by the size of the ceramic powder particles and by the homogeneity of their mutual coordination but similarly strongly by the state of the crystal lattice: with different cation disorder at fixed stoichiometry ($n = 1$) the sintering temperatures may differ by as much as 200 °C at constant powder particle size and equal homogeneity of the green bodies. Additionally, the impact of stoichiometry was investigated over the range between $n = 1$ and $n = 3$ with retarded reactive sintering at moderately increased Al_2O_3 concentrations but promoted densification of alumina-rich compositions. Taking advantage of the observed effects, sintered spinel ceramics were derived by reactive sintering of undoped MgO/Al_2O_3 mixtures resulting in an in-line transmittance which equals spinel single crystals of similar composition from 200 nm wave length up to the IR range.

Keywords: Spinels (MgO, Al2O3); Sintering; Optical properties

1. Introduction

Magnesium aluminate spinel is a candidate for sintered windows, domes and lenses for ultraviolet (UV), visible (VIS), and infrared (IR) applications. As in all transparent materials the residual porosity has to be <0.01% when the target is a high transmittance and a glass-like appearance. Obviously, this extreme challenge needs raw powders with a high sintering activity, i.e. with small particles. Additionally, the sintering densification of a given high-purity powder with particles <300 nm is significantly promoted by processing approaches which improve the homogeneity of the mutual particle coordination in the green bodies. By such improved processing, the sintering temperature of Al_2O_3 was reduced from about 1500 °C to <1300 °C[1] and, later on, to 1130 °C.[2] Evidence for the *homogeneity* as the origin of this big effect comes from measurements of improved (more narrow) pore size distributions of the green bodies.[2,3] A comprehensive summary of the roles of particle size and of homogeneity was given previously (e.g. by Fig. 9 in Ref. 4).

The optimization of *transparent* ceramics with their special challenge to eliminate not last tenths but the one last hundredth of 1% of residual porosity needs a sufficiently sensitive record of this extreme densification in the last stage of sintering. A commonly accepted tool is the *in-line* transmittance of finally sintered, ground and polished samples. Eventual scattering losses depend, however, not only on the *porosity* but also on the ratio of the typical *size* of the pores to the applied wave length. For 1 mm thin spinel Fig. 1 demonstrates the general understanding that (i) the most detrimental pore size scales with the wave length and that (ii) the scattering power of nanopores diminishes at larger wave lengths.[5] On the other hand, Fig. 1 also shows that even at longer (IR) wave lengths only *very thin* windows will tolerate smaller pores ≤100 nm for imaging applications. Altogether, Fig. 1 shows that the most sensitive check for last nanoscale pores will be the in-line transmission measured through *thicker* windows at *shorter* wave lengths.

Unfortunately, most cubic oxide lattices preferred for transparent ceramics exhibit structures which are not as well-defined and stable as that of, for example, corundum. It is, therefore, highly probable that (i) the sintering performance and (ii) the inherent transmittance of such ceramics will be influenced by differences in the real structures of the crystals. Published work on this issue is, however, rare and often inconsistent. For Mg–Al spinel ($MgO{\cdot}nAl_2O_3$) one early report[6] showed an *increased* diffusion of oxygen (the rate-controlling species[7]) when n increases from unity to 1.8 and on to 3.5. Enhanced diffusion should promote sintering with a positive influence on the final transmission, but another investigation published in the same year

* Corresponding author. Tel.: +49 351 2553 7538; fax: +49 351 2553 7600.
E-mail address: Andreas.Krell@ikts.fraunhofer.de (A. Krell).

0955-2219/$ – see front matter © 2012 Elsevier Ltd. All rights reserved.
doi:10.1016/j.jeurceramsoc.2012.02.054

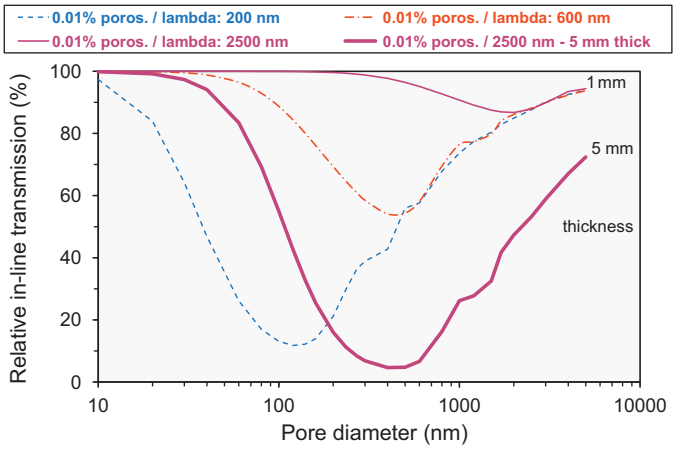

Fig. 1. Mie calculation of the influence of pore size on the transmittance of $MgO{\cdot}Al_2O_3$ spinel windows with different thickness at 200, 600, and 2500 nm wave length.

did not reveal a significant benefit of $n = 1.8$ compared with e.g. $n = 1.1$.[8] In contrast, a recent Japanese patent application claims an optimum transmission (with minimum scattering losses) for compositions with $n = 1.05–1.30$[9] and refers to lower transmittance data at lower and at higher n. The latter is in a partial agreement with Dericioglu et al.[10] who reported an increased UV–vis *absorption* of Al-rich compositions with higher n-values of 1.5 and 2 while there was, surprisingly, no influence on the sintering densification. On the other hand, the claim of an optimum transmission at $n = 1.05–1.30$ appears surprising since for similarly increasing Al contents ($n = 1–1.5$) Ting et al. observed a *retarded* densification during reactive sintering of MgO/Al_2O_3 mixtures in air as in a vacuum.[11] Probably, these numerous discrepancies cannot be attributed to one single feature such as e.g. the composition. It has, however, to be noted that the most complete elimination of last pores (indicated by the highest transmission of sintered spinel ceramics at short wave lengths) was achieved with compositions close to a 1:1 stoichiometry ($MgO{\cdot}nAl_2O_3$ with $n = 1$) by two Japanese groups which published their results in the form of patent applications only:

- Ikesue[12] claims a transmittance (not explicitly termed "in-line") of ~76% for 10 mm thick (!) samples at 193 nm wave length, achieved by conventional vacuum pre-sintering (1550 °C/2 h) and subsequent hot-isostatic pressing (HIP, 1780 °C/2 h) of pressed bodies made from some powder with 100 nm particle size and a "spinelization rate" of 90% (prepared by incomplete calcination of unknown precursors) with a doping additive of 0.3% MgF_2 and 0.3% AlF_3.
- For the same wave length of 193 nm Tanaka et al.[13] report an in-line transmission of 73% for 4 mm thick samples (=equivalent to about 61% at 10 mm thickness) after *reactive* hot-pressing (1550 °C/2 h) and subsequent HIP (1800 °C/2.5 h) of an Al_2O_3/MgO mixture with a conventional doping additive of 4% LiF.

It is worth noting that both these outstanding results were achieved by quite common sintering regimes and a preference of compositions close to a 1:1 stoichiometry using, however, *reactive* processes (instead of starting with completely pre-calcined spinel powders) supported by doping additives.

It has to be emphasized that neither Ikesue[12] nor Tanaka et al.[13] reveal a preference for extremely fine (nanoscale) raw powders <100 nm. This is in agreement with another investigation which has demonstrated that spinel powders with

- particle sizes of 50–60 nm may decrease the sintering and HIP temperature to less than 1400 °C improving the mechanical performance at a high *visible* and *near IR* in-line transmittance but associated with a deterioration of the transmission <400 nm caused by nanopores that survive the HIP process, whereas
- the use of *coarser* powders (~120 nm) reduces the amount of such nanopores by one order of magnitude.[14]

Regarding these previous results[12–14] the present investigation was aimed at answering the following questions:

- Can spinel lattices with identical stoichiometry but synthesized by different approaches give rise to a significantly different sintering densification as a consequence of differences in their lattice structures?
- Can, therefore, a *reactive* sintering of MgO/Al_2O_3 powders (eventually with coarser particle sizes ≥100 nm) provide an advantage for the elimination of last pores compared with the sintering of pre-calcined spinel powders?
- Does the *stoichiometry* influence (i) the *sintering* densification and (ii) the *inherent* transmittance of spinel lattices?
- Are doping additives (which may initiate specific *absorptions* or precipitations with *scattering* losses) imperative for minimizing the amount of residual porosity in transparent spinel ceramics prepared by pressure-assisted sintering?

2. Experimental procedure

2.1. Raw materials

With the recent experience of *less* nanopores in those transparent windows prepared from the *coarser* spinel powders (with about 120 nm particle size),[14] magnesia and corundum powders with similar or even larger particles were preferred for the present investigations of reactive sintering with variations of the stoichiometry (Table 1). For the comparative *spinel* powder the equivalent particle size of 120 nm derived from the specific BET surface was confirmed by laser scattering (Mastersizer 2000, Malvern Instruments, USA) after ultrasonification of the powder in water with sodium hexametaphosphate dispersant which resulted in a median value of 150 nm (=close to the BET-derived value and indicating, thus, a low degree of agglomeration).[14] A similarly low degree of agglomeration was indicated for corundum powders of similar particle size e.g. by a median value of 150 nm (Mastersizer) and 116 nm BET-equivalent size of the

Please cite this article in press as: Krell A, et al. Influence of the structure of $MgO{\cdot}nAl_2O_3$ spinel lattices on transparent ceramics processing and properties. *J. Eur. Ceram. Soc.* (2012), doi:10.1016/j.jeurceramsoc.2012.02.054

Table 1
Raw powders for reactive sintering investigations compared with a commercial spinel powder of similar granulometric characteristics. The derived equivalent particle size (=6/(ρ·S_{BET}) with ρ – density, S_{BET} – specific surface) assumes spherical particles and a mono-size distribution.

Materials	Specific surface (BET)	Equivalent particle size
α-Al_2O_3	13.5 m^2/g	110 nm
	13.0 m^2/g	116 nm
	9.2 m^2/g	163 nm
	4.9 m^2/g	305 nm
MgO	8.6 m^2/g	195 nm
	8.2 m^2/g	205 nm
Comparative: commercial spinel	13–15 m^2/g	120 nm

powder in the second line of Table 1. The purity of all powders was >99.98%.

In order to provide shaped samples for sintering experiments starting with *almost equal* particle *sizes* and an equal *homogeneity* of the mutual particle coordination in the green bodies, additional spinel powders were synthesized by different approaches[15] which cannot be outlined here. Most of these powders were prepared from different dissolved inorganic or organic precursors whereas two tests dispersed a 50 nm MgO or a 116 nm corundum powder, respectively, in the solution of the second component which was then precipitated on the surfaces of the suspended oxide particles. After calcination most of these powders exhibited high specific surfaces >50 m^2/g. Fundamental difficulties of a correct assessment of size distributions of nanoscale spinel powders and strategies for a solution of these measuring problems were discussed in a previous paper.[14] Focused on consequences *for sintering* the present investigation classifies these powders by their specific BET surfaces and derived "equivalent" particle sizes (Table 2) and by the resulting *pore size* distributions of the green bodies (Fig. 2a). These pore size distributions are more directly related to sintering than *powder* particle size distributions which are modified significantly by following processing (Table 2) and frequently are incorrectly recorded by common dynamic or static laser scattering approaches.[14]

2.2. Powder processing, shaping and sintering

The degree of dispersion of the spinel powders and, for reactive sintering, of the MgO/Al_2O_3 mixtures was improved by several hours of ball-milling followed by drying, granulation, uniaxial pre-pressing at about 50 MPa, and subsequent cold isostatic pressing (CIP) at 700 MPa as described previously.[14] In most of the investigations no sintering additives were used in order to investigate the original sintering ability of the powders without secondary influences.

After careful burnout of organic additives (0.2 K/min up to completed burnout), all samples were pre-sintered in air up to closed porosity (about 95-98% of relative density) followed by HIP in argon for 8–15 h with a pressure of 200 MPa.[14]

For comparison, a few samples were hot-pressed with a 4% LiF additive at 1650 °C with an isothermal hold of 5 h.

2.3. Measurements

The achieved degree of homogeneity of the particle coordination in the green state was evaluated by measuring the pore size distributions[3] after outgassing at 800 °C. The equipment used here (Autopore IV-9500, Micromeritics Instrument Corp., Norcross, GA) derives the pore diameter assuming cylindrical pores (Washburn equation) with a constant contact angle of 130° (mercury intrusion). The lower bound of recorded pore sizes was 6 nm for the present measurements, and an upper bound of 500 nm was considered as a limit between "real" pores and larger defects, which were excluded from the pore size evaluation.

Green densities were measured geometrically and checked by the total intrusion volume of mercury porosimetry. These data together with the *wide range* of recorded pore sizes enable a reliable assessment of those features of homogeneous or aggregated particle coordination which influence the sintering densification.[3]

Table 2
Raw materials and granulometric data of synthesized spinel powders[15] and green compacts prepared for comparative sintering investigations of spinel bodies with similar green structure but different synthetic origin. Same meaning of equivalent particle size as in Table 1.

	Raw materials	Synthesized powders:			Green bodies:		
		Temperature of calcination	Resulting specific surface (BET)	Equivalent particle size	BET	Particle size	Relative density
A-1	Different combinations of	1100 °C	81 m^2/g	21 nm	70 m^2/g	24 nm	59%
A-2	Mg and Al alkoxides[15]	1100 °C	19 m^2/g	88 nm	27 m^2/g	61 nm	60%
N-1	Al and Mg nitrates	900 °C	n.d.		61 m^2/g	27 nm	56%
N-2		1000 °C	52 m^2/g	32 nm	63 m^2/g	27 nm	57%
MgO/Al-A	MgO (50 nm equivalent to BET) dispersed in solution of Al alkoxide	1100 °C	65 m^2/g	26 nm	68 m^2/g	25 nm	57%
Al_2O_3/Mg-A	Al_2O_3 (116 nm equivalent to BET, 150 nm median size by Mastersizer) dispersed in solution of Mg alkoxide	800 °C	14 m^2/g	112 nm	17 m^2/g	99 nm	51% (?)

Please cite this article in press as: Krell A, et al. Influence of the structure of MgO·$n$$Al_2O_3$ spinel lattices on transparent ceramics processing and properties. *J. Eur. Ceram. Soc.* (2012), doi:10.1016/j.jeurceramsoc.2012.02.054

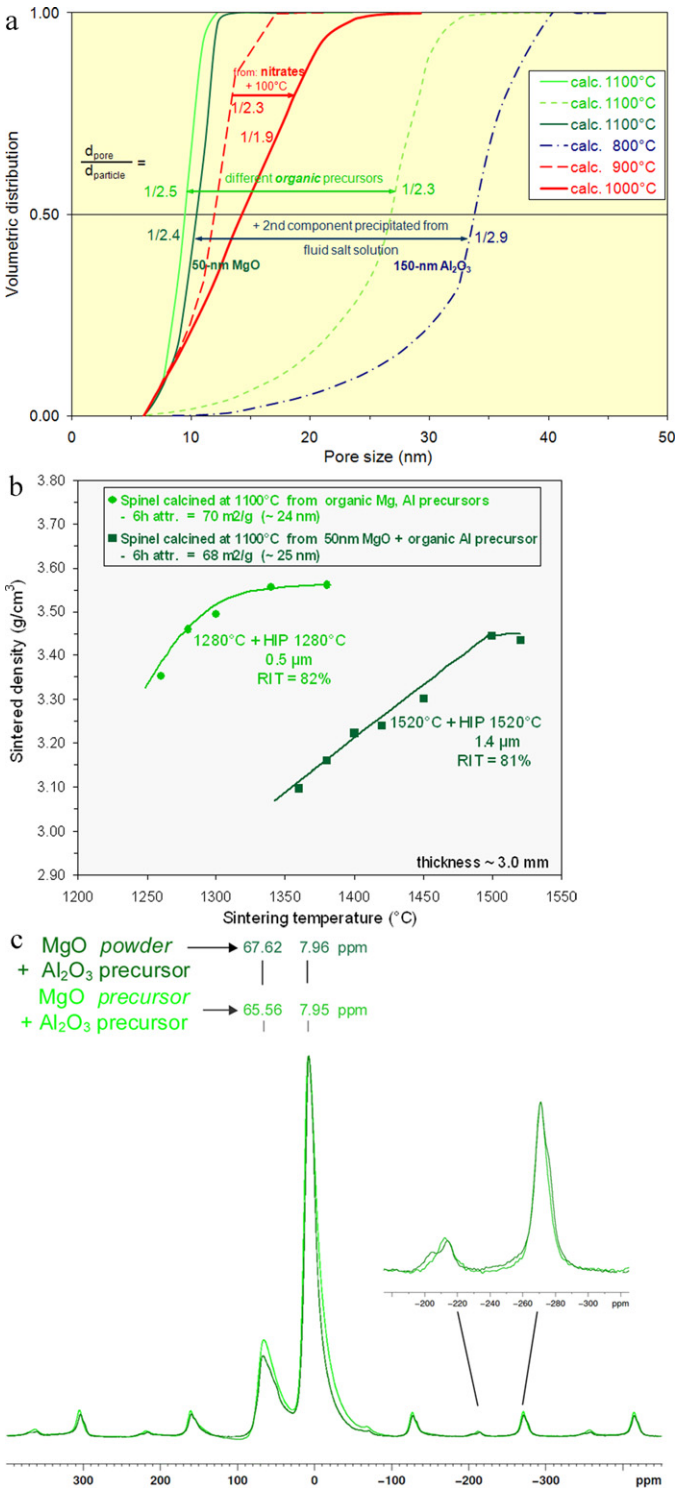

Fig. 2. (a) Pore size distributions of green bodies (annealed 800 °C) made of differently synthesized[15] spinel powders (Table 2). (b) Sintering performance (in air, 2 h isothermal hold at indicated temperatures) of the two green samples with the finest pore size distributions in (a) (A-1, MgO/Al-A in Table 2). Inserts to the curves give the measured average grain sizes and the real in-line transmissions (at wave length 640 nm) after sintering + HIP. (c) NMR spectra of two of the differently synthesized spinel powders A-1 and MgO/Al-A (Table 2) prepared for green bodies (a) with the sintering performance displayed by (b). Equal calcination at 1100 °C with completed conversion to spinel. The ratio of the peaks at 7 and at about 67 ppm represents the amounts of Al species on regular Al sites (AlO_6 octahedra) and of "displaced" Al on tetrahedral sites (AlO_4).

The density of sintered parts was measured following Archimedes' principle with a careful record of the temperature (i.e. of the density) of the de-ionized and de-aerated water.

For relative densities >99.9%, the elimination of last pores was assessed by two different transmission measurements of polished disks: the spectroscopic "in-line" performance over the UV and the extended visible range was recorded by a Cary 4000 spectrometer (Varian Inc., Mulgrave, Vic., Australia) and compared with the total transmission measured by the same equipment with an integrating Ulbricht sphere. The spectroscopic measurements were completed for the IR range with a Spectrum 400 (Perkin-Elmer, Waltham, MA, USA).

The spectroscopic results of polycrystalline (sintered) spinel samples were compared with two (1 1 1) single crystals:

- An $MgO{\cdot}nAl_2O_3$ crystal with $n = 1$ was obtained from Leibniz IKZ Berlin (Germany) and
- another crystal with $n \approx 2.7$ was purchased from Saint-Gobain Crystals (Milford, NH, USA).

Both crystals exhibited a similar purity with about 25–30 ppm Ca, 2–3 ppm Cr, 2–3 ppm Fe, and 1–2 ppm Zn. Additional reference comes from two *published* spectra (not measured in our laboratory) of Saint-Gobain crystals with $n = 1$.[16,17]

In order to investigate eventual correlations of the observed sintering performance with features of the spinel lattices the study had to address the state of these lattices *at the beginning* of sintering. Solid-state ^{27}Al MAS-NMR (magic-angle spinning nuclear magnetic resonance spectroscopy) conducted with an Avance^{TM} 400 MHz WB spectrometer (Bruker Corp., Billerica, MA, USA) was used to characterize differently synthesized virgin spinel *powders* after calcination at 1100 °C (where X-ray diffraction indicated a completed conversion to cubic spinel). Comparative measurements were performed with the materials of transparent spinel bodies of different stoichiometry *after* sintering and HIP.

3. Results

3.1. Influences of different spinel lattices with n = 1 on the sintering densification

With only 1/8 of the available tetrahedral sites occupied by Mg^{2+} and 1/2 of the octahedral sites occupied by Al^{3+} species the $MgAl_2O_4$ crystal exhibits a significant propensity for cation exchange and interstitial defects even at fixed stoichiometry.[18] With the common assumption of an *equal* disorder of Al and Mg species (in Kröger–Vink notation: $Mg^x_{Mg} + Al^x_{Al} \rightarrow Mg'_{Al} + Al^{\bullet}_{Mg}$) the degree of inversion is described by a parameter i which is defined by $(Mg_{1-i}Al_i)[Mg_iAl_{2-i}]O_4$ (curved brackets refer to the tetrahedral and square brackets to the octahedral sites). With this definition the relationship between the inversion parameter i and the ratio of Al species on "disordered" tetrahedral AlO_4 and on "normal" octahedral AlO_6 sites is $\{AlO_4\}/\{AlO_6\} = i/(2-i)$.

The *propensity* for cation exchange does, however, not imply any basis for a forecast of *quantitative* consequences for

diffusion (on sintering) and other processes (e.g. light transmittance). In order to separate *lattice* effects from other influences on sintering densification comparative tests have to be performed with green spinel bodies which definitely associate

- *different* real structures of their lattices (preferably at *same* stoichiometry) with
- *equal* particle sizes, particle size distributions, dispersibilities and homogeneities of the particle coordination.

This target was matched by two of the green bodies which were cold-isostatically pressed from differently synthesized[15] spinel powders (A-1 and MgO/Al-A in Table 2). Fig. 2a summarizes the pore size distributions of all of these green bodies; typical green densities (Table 2) were 56–60% of the theoretical value (3.57–3.58 cm^3 measured after HIP). After equal calcination at 1100 °C and with equal processing (milling, shaping) the two grades of green samples made of

- the finer of the two spinel powders derived from organic MgO and Al_2O_3 precursors (A-1) and, respectively, of
- a spinel prepared by precipitation of the Al-component on the surface of a 50-nm MgO powder (MgO/Al-A)

exhibited single-phase spinel (X-ray analysis) with (i) a nominally equal 1:1 starting *stoichiometry*, (ii) same average *particle sizes* (indicated by specific surfaces of 68 and 70 m^2/g measured on the green bodies after milling of the powders, compaction and removal of organic additives - Table 2), (iii) a same *homogeneity* of the particle coordination (same narrow width of the pore size distributions and an almost equal ratio of pore size to particle size of (1/2.5)–(1/2.4)), and (iv) a similar specific volume of pores ≤125 μm (0.165–0.170 ml/g) and similar green densities (57 and 59%). Also, both spinel powders were subjected to the same milling procedure such that lattice differences caused by different mechanical activation[19] are excluded.

Thus, if with fixed composition the sintering performance were governed by particle size and homogeneity only, these two grades should exhibit a similar sintering densification. In fact, however, Fig. 2b gives evidence of a completely different sintering performance with a big temperature difference of about 200 °C.

NMR spectra of the pre-calcined spinel powders were recorded in order to explain this surprising behavior (Fig. 2c). In fact, the different syntheses of these raw powders do not completely exclude the possibility of some compositional change in the course of the chemical preparation, and such change could have contributed to the different NMR spectra in Fig. 2c. Nevertheless, these NMR results highlight the *one* obvious difference between these two spinel powders: the spinel with enhanced sintering activity (i.e. the powder derived from organic MgO and Al_2O_3 precursors in a way where the spinel lattice was completely formed from the molecular precursors) exhibits a higher degree of disordered Al species than the spinel which was "re-" formed from the template of a pre-existing cubic MgO powder. For this latter grade the split satellite peak at −210 ppm additionally points to an eventual residual content of a second phase (probably MgO or some Al_2O_3 phase).

With this impact of spinel lattices of different origin on the sintering densification displayed by Fig. 2b it is highly probable that an in situ formed (during the first stage of *reactive* sintering) spinel could exhibit a significantly different sintering performance compared with pre-calcined spinel powders. As a check of this idea Fig. 3a compares the pressureless sintering (in air) of

- green bodies prepared from a 120 nm *spinel* powder (after 2 h of milling and shaping as outlined above) with
- the *reactive* sintering of green *composite* bodies which were manufactured from an equally (2 h) processed MgO/Al_2O_3 mixture with an originally *larger* average particle size than the spinel (the particle size of the alumina component was similar as the spinel, but the 195 nm MgO powder was much coarser).
- Additionally, Fig. 3a includes the reactive sintering data of MgO with a still coarser corundum powder (163 nm) after 6 h of milling.

For a clear understanding it has to be noted that X-ray analyses indicated a completed spinel formation in the present reactive

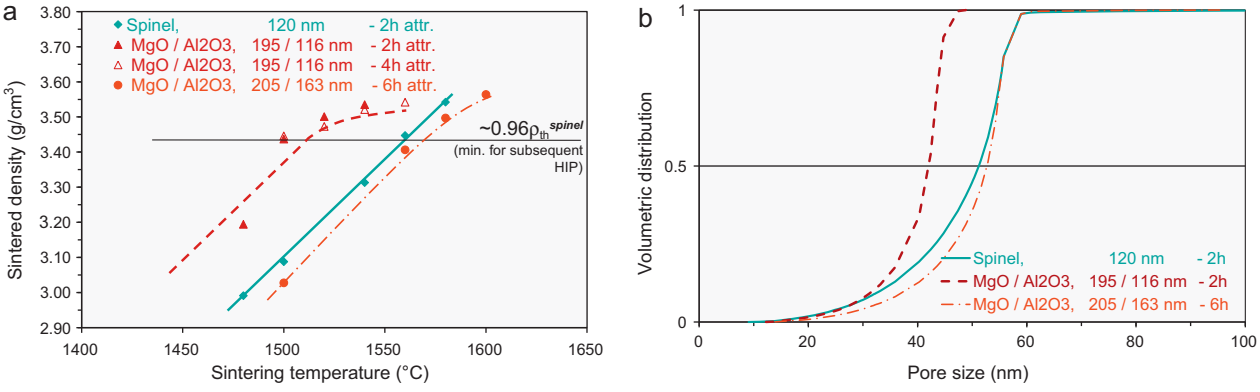

Fig. 3. (a) Improved densification on *reactive* sintering of MgO/Al_2O_3 bodies (starting molar composition equivalent to $MgO:Al_2O_3 = 1:1$) compared with the sintering performance of bodies prepared by equal powder processing and shaping of a commercial spinel powder with same stoichiometry and an average particle size of 120 nm. (b) Pore sizes of green bodies (after burn-out of organic additives at 800 °C) used for the sintering study of (a).

Please cite this article in press as: Krell A, et al. Influence of the structure of $MgO{\cdot}nAl_2O_3$ spinel lattices on transparent ceramics processing and properties. *J. Eur. Ceram. Soc.* (2012), doi:10.1016/j.jeurceramsoc.2012.02.054

sintering tests with 1:1 stoichiometry up to about 1100 °C or below. Therefore, *all* data points in Fig. 3a refer to a state of 100% spinel independent of the different raw materials.

Fig. 3a confirms the assumed benefit of *reactive* sintering: after 2 h of identical milling the composite bodies which were shaped from a mixture of 195nm MgO and 116 nm α-Al_2O_3 come to the state of closed porosity (=pre-requisite for subsequent cladless HIP) at a temperature which is 50 K lower than observed for the bodies made of the 120 nm spinel powder. This benefit disappears apparently only with the use of a still coarser corundum: in fact, with extended 6 h of milling even these bodies reproduce the sintering behavior of the originally much finer (!) spinel powder.

Since, however, sintering responds (i) to the particle sizes in the *processed* green bodies (*not* to the *original* size distributions of the raw powders) *and* (ii) to the *homogeneity* of particle coordination[3,14] *the cause* of the improved densification on reactive sintering (Fig. 3a) is not obvious without additional checks. Therefore, the pore size distributions are displayed in Fig. 3b which reveals a surprising effect: equal milling (for e.g. 2 h) influences the (originally coarser) MgO much stronger than the spinel powder and brings, thus, the whole MgO/Al_2O_3 mixture to a state where the shaped green composite bodies exhibit a *finer* pore size distribution than that of the spinel body – despite the *originally* much coarser particles of this MgO/Al_2O_3 mixture.

Therefore, Fig. 3a and b do neither exclude nor confirm an increased activity *of the lattice* of the in situ formed (by solid-state MgO/Al_2O_3 reaction) new spinel on reactive sintering. An enhancement of the sintering densification by improved diffusion of the "new" spinel lattice becomes, however, clear when the reactive sintering of Fig. 3a is compared with the results of Fig. 2a and b:

- The green bodies prepared from the pre-calcined spinel (synthesized by a templating cubic MgO powder and an Al-precursor) sintered to closed porosity at about 1500 °C (Fig. 2b) starting from a spinel particle size of about 25 nm and a median pore size of 11 nm (Fig. 2a), whereas
- a *similar* sintering temperature is displayed by Fig. 3a on reactive sintering of the composite bodies made of *much coarser* 195 nm MgO and 116 nm Al_2O_3 particles and with about 40 nm median pore size. With reference to these *different* (by a factor of 4 and more) particle and pore sizes the similar sintering temperatures are a clear indication of the higher diffusional activity of the in situ formed "new" (probably highly defective) spinel during reactive sintering.

An information about the impact of the temperatures of reactive sintering and HIP on the concentration of antisite defects comes from a comparison of the NMR spectrum of the *sintered* and HIP-ed *compact* with 1:1 stoichiometry in Fig. 4a (lower curve) with the two spectra of differently synthesized but equally calcined and processed spinel *powders* in Fig. 2c. At same 1:1 stoichiometry, the ratio of the peaks at 64.68 ppm to the peaks at 7 ppm in Fig. 2c is $\{AlO_4\}/\{AlO_6\} = 0.21$ for the MgO-derived powder and still higher (0.26) for the other powder with the improved sintering shown in Fig. 2b. This peak ratio is, however, *lower* (0.18) for the reactively sintered body with same 1:1 stoichiometry in Fig. 4a in some contrast to its high reactive sintering activity discussed above. It has, therefore, to be concluded that the high temperatures of pre-sintering (1570 °C) and of HIP (1750 °C) have given rise to some decrease of the concentration of antisite defects at constant stoichiometric composition.

The small but significant splitting of the major NMR peak of the stoichiometric spinel in Fig. 4a (at 8.45 and 4.16 ppm) was seen in previous NMR records of – apparently single phase and stoichiometric – $MgAl_2O_4$ spinel[20–22] and is attributed to a second-order nuclear-quadrupole interaction.[23,24] A formal computer simulation of the spectrum including the first-order contribution to the spinning side bands as well as the contribution of the second-order interaction to the central transition was performed by Maekawa et al.[22] It turned out that a successful fit of the spectra has to take into account *two different* types of AlO_6 octahedra which are distinguished by a different degree of asymmetry (asymmetry parameter $\eta = 0.26$ and 0.4, respectively).[22] Apparently, η and the shape of this doublet are not directly correlated with the cation disorder in spinel: in Fig. 4a the peak at about 4 ppm is higher for the stoichiometric spinel ($n = 1$) with the *lower* disorder (a smaller peak at 69 ppm attributed to AlO_4) whereas for natural spinel (with an inversion <0.1) Maekawa et al.[22] observed an increase of this part of the doublet associated with *increasing* disorder.

3.2. Role of stoichiometry during reactive sintering

With the above results of significantly different cation disorder in spinel lattices originating from different syntheses it is not a surprise to find that in Fig. 4a a larger variation of the *composition* $MgO{\cdot}nAl_2O_3$ ($n = 1$–2.5) gives rise to NMR spectra which exhibit a bigger difference of the concentration of displaced Al species on sites of 4-fold coordination than observed in Fig. 2c for powders of different syntheses but similar composition. The high degree of cation disorder in the Al-rich sintered body is indicated in the spectra of Fig. 4a not only by a higher ratio of the AlO_4/AlO_6 peak *heights* (~0.27 at $n = 2.5$ vs 0.18 at $n = 1$) but additionally by a much larger *width* of the AlO_4 peak of this material compared with the stoichiometric one. This increase of cation disorder in Al-rich spinel with $n \sim 3$ is known for at least 35 years[25] and is easily understood: compared with the lattice at $n = 1$ "alumina-rich" spinel is, in fact, a *low-Mg* structure with a concomitant rise in the concentration of both cation vacancy species[26] and with the consequences of (i) stimulated site exchange processes which increase the occupation of tetrahedral sites by Al species[11,27] and (ii) with a decreasing lattice parameter (Fig. 4b, incorporating a standard reference[28]). A more profound (atomistic) interpretation of the relationship between increasing inversion and decreasing lattice parameter was recently proposed by Shukla et al.[29]

The expected consequences for the sintering densification are seemingly clear: irrespectively of some controversial data in the literature the smaller lattice parameter of Al-rich spinel should retard the diffusion of oxygen (as the largest and, therefore, rate-controlling species[7]). In fact, the present sintering results

Please cite this article in press as: Krell A, et al. Influence of the structure of $MgO{\cdot}nAl_2O_3$ spinel lattices on transparent ceramics processing and properties. *J. Eur. Ceram. Soc.* (2012), doi:10.1016/j.jeurceramsoc.2012.02.054

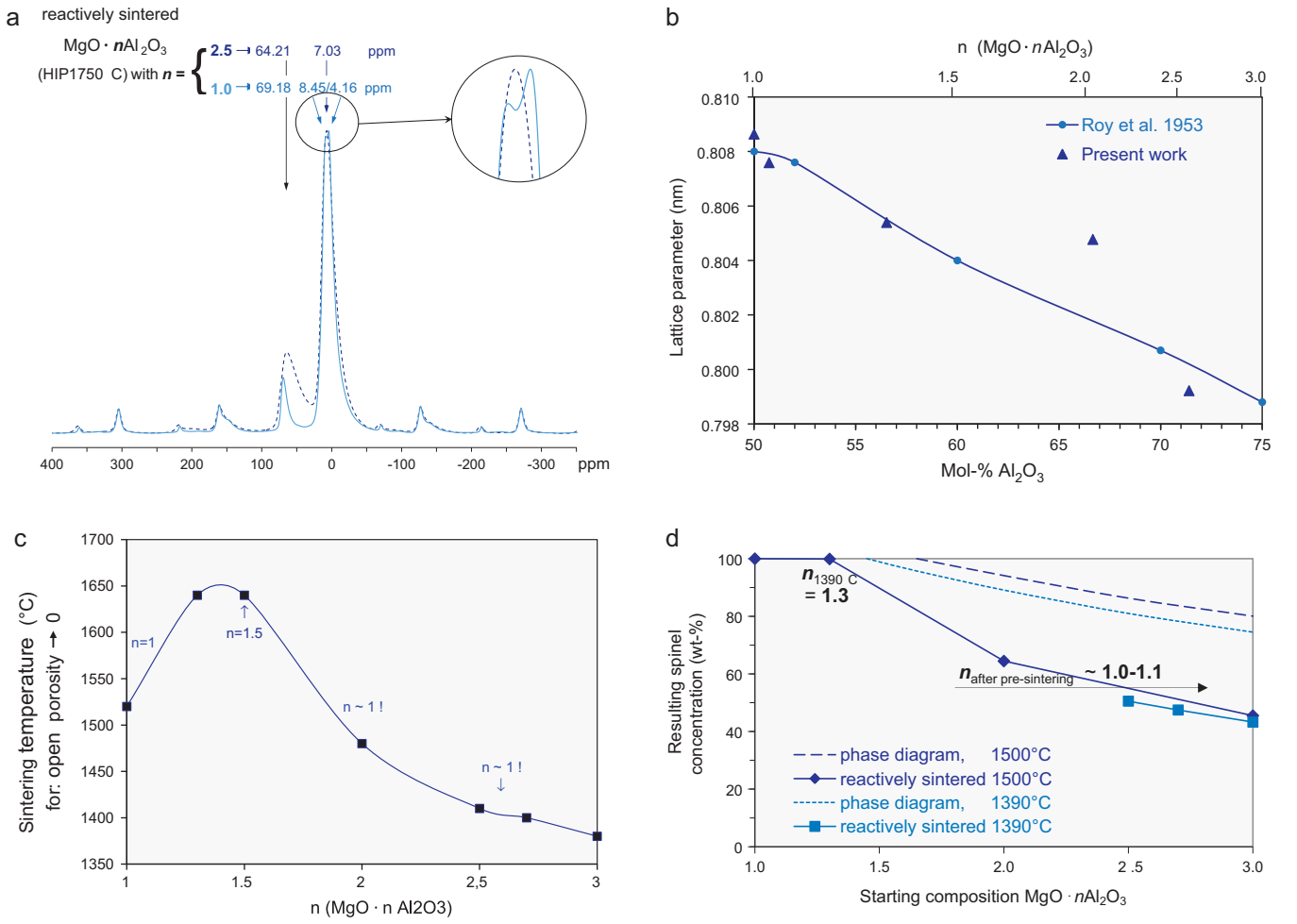

Fig. 4. (a) NMR spectra of two reactively sintered (from 205 nm MgO + 163 nm Al_2O_3; 1570 °C) and HIP-ed (at 1750 °C) spinel bodies with different compositions. (b) Lattice parameters (determined by X-ray diffraction) of spinel with increasing Al_2O_3 content. The measuring accuracy is about ±0.000015 nm. (c) Reactive sintering (air, 2 h isothermal hold) of 195 nm MgO with 116 nm Al_2O_3: influence of the starting composition on the temperature for closure of pores (at about 96% relative density) and on the resulting composition of the reactively formed spinel phase. The *x*-axis refers to the starting MgO/Al_2O_3 *powder* ratios whereas inserts give the composition of the *spinel* phase formed during the sintering process. (d) Reactively generated spinel contents and spinel compositions depending on starting compositions (195 nm MgO, 116 nm Al_2O_3) after 2 h isothermal pre-sintering at 1390 °C and 1500 °C, respectively, compared with expectations from phase diagram.[28]

confirm this expectation *as far as* Al-*rich* spinel is really formed on reactive sintering, and this last condition makes the final consequences of compositional changes rather complex changing from "retard" to "promote" depending on *n* (explaining some controversial reports in the literature which were limited to more narrow ranges of the composition): as displayed by Fig. 4c, the temperature required for the closure of open porosity

- *increases* for moderately increased alumina contents ($n = 1–1.5$, in this range in agreement with Ting et al.[11] and as expected above) but
- shifts for higher *n* to *lower* values than observed on reactive sintering of same MgO and Al_2O_3 powders with 1:1 stoichiometry.

This turning behavior at $n \sim 1.5$ (Fig. 4c) can, however, not be attributed to an eventually changing diffusion in spinel lattices with higher alumina contents because, surprisingly, all data points in Fig. 4c for $n > 1.5$ do *not* refer to sintered Al-rich spinel but to nearly stoichiometric $MgAl_2O_4$: X-ray measurements of the lattice constants showed that by reactive sintering of different *starting* compositions of MgO/α-Al_2O_3 with an increasing amount of Al_2O_3

- single phase and increasingly Al-rich spinel with MgO/α-Al_2O_3-ratios close to the starting mixtures was obtained for compositions with $n = 1–1.5$ only (with increasing pre-sintering temperatures of 1520–1650 °C)
- whereas with starting compositions with $n > 1.5$ only spinel with $n \sim 1$ was formed during the *promoted* by Al-rich compositions reactive pre-sintering at temperatures <1500 °C. Disregarding kinetic effects addressed by the discussion below this observation seems to be in conflict with known phase diagrams which at 1300–1500 °C and for a state of equilibrium allow single phase spinel with $n = 1.3–1.6$ (as e.g. given by Roy et al.[28]). This surprising formation of 1:1 spinel in these Al-rich pre-sintered bodies is, of course, associated with an excess of residual corundum and with an equivalent spinel content not

Please cite this article in press as: Krell A, et al. Influence of the structure of MgO·nAl_2O_3 spinel lattices on transparent ceramics processing and properties. *J. Eur. Ceram. Soc.* (2012), doi:10.1016/j.jeurceramsoc.2012.02.054

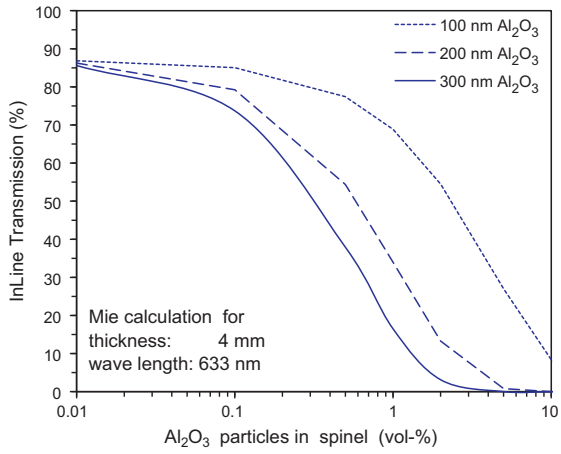

Fig. 5. Influence of small amounts of Al_2O_3 grains in spinel on the in-line transmittance of 4 mm thick windows.

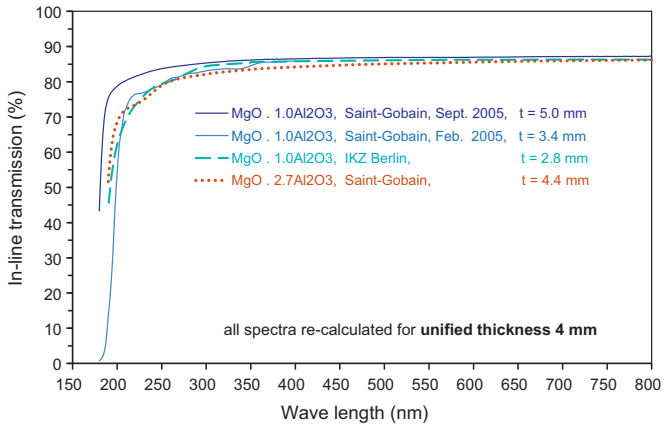

Fig. 6. Transmission spectra of $MgO{\cdot}nAl_2O_3$ single crystals with different compositions and different original thicknesses (unified here for one intermediate thickness t of 4 mm; the original spectra of the Saint-Gobain crystals with $t = 5.0$ mm and $t = 3.4$ mm are derived from Refs. 16,17).

only <100% but below the concentration expected at these temperatures from the phase diagram (Fig. 4d). The residual alumina was incorporated into the primary $MgO{\cdot}Al_2O_3$ lattice at higher temperatures of the subsequent HIP process only.

One consequence of the consumption of the residual Al_2O_3 at higher temperatures only is that the *low* temperatures enabled by reactive pre-sintering of alumina-rich compositions with $n > 1.5$ (Fig. 4c) cannot be used for the preparation of *highly transparent* (single phase) spinel ceramics *at low* HIP temperatures that produce fine grain sizes: Fig. 5 illustrates that despite the small difference between the refractive indexes of Al_2O_3 (1.765 at 600 nm wave length) and spinel (1.715 at 600 nm) as few as 0.1–0.5 vol% of Al_2O_3 grains in spinel will intolerably deteriorate the in-line transmittance of the transparent ceramic.[5]

We have, however, to note that this restriction does *not* exclude an eventual contribution of the promoted by a higher Al content sintering densification *not only* during pre-sintering (Fig. 4c) but also on the final elimination of last nanopores during HIP at the higher temperatures required for the consumption of residual alumina.

3.3. Spectroscopic results

Fig. 6 compares the transmission spectra of different magnesium aluminate single crystals published in the literature[16,17] or measured in the frame of the present investigation (for this figure all original data were re-calculated for one intermediate unified thickness of 4 mm). The important message is that *different growing* conditions influence the visible and the UV transmittance just as or even more strongly as observed for the widest variations of the composition between $n = 1$ and $n \approx 3$ (with increasing deviations at shorter wave lengths). Thus, with the data of single crystals (Fig. 6) a larger impact *of the composition* on the inherent UV and visible transmittance has to be denied.

The UV–vis and the IR parts of the transmission spectra of the prepared polycrystalline sintered spinel ceramics are presented by Fig. 7a and b. The decrease of the UV transmittance at wave lengths <300 nm was much smaller for the *reactively* sintered bodies than for samples made of *spinel* powder *if* the employed MgO and Al_2O_3 powders were *coarser* than the successful *spinel* powders of a former[14] investigation. The best transmission was achieved with starting particles of about 150–200 nm and with a composition of $n = 2.5$: the in-line spectrum of these reactively pre-sintered and HIP-ed bodies matches closely that of a single crystal with similar composition.

In Fig. 7a the declining spectrum <300 nm of the bodies made of commercial *spinel* powder suggests scattering losses as modeled by the Mie calculation of the transmission of spinel with 0.005–0.01% of 40 nm small pores (Fig. 8 in Krell et al.[30]). Therefore, the elimination of such last pores was one of the targets of the present work. An improved *reactive* sintering densification was indicated by Fig. 3a, and now in Fig. 7a it is the coincidence of the in-line and the total transmissions of these reactively sintered samples made with the 163 nm Al_2O_3 (composition with $n = 2.5$) which gives evidence that the improved transmittance of this material was, in fact, achieved by minimizing the amount of nanopores and of associated scattering losses.

Apparently, this strategy works well with starting alumina and magnesia powders which originally are coarser than the typically used commercial spinel powders. With Figs. 2b and 3a and b it is assumed that this effect is partially caused by

(i) an improved inherent diffusion and sintering densification of the "new" spinel lattice formed in situ during the first stage of reactive sintering and
(ii) by the stronger impact of milling on the MgO/Al_2O_3 mixtures enabling smaller average pore sizes of the shaped green bodies with coarser MgO/Al_2O_3 powders than possible by the same processing with finer spinel powders (Fig. 3b).

Fig. 7a demonstrates, however, an upper limit for this benefit of coarser MgO or Al_2O_3 raw powders: the coarsest of the MgO/Al_2O_3 mixtures investigated by Fig. 3a and b contributed to the best transmittance in Fig. 7a, but with a still bigger

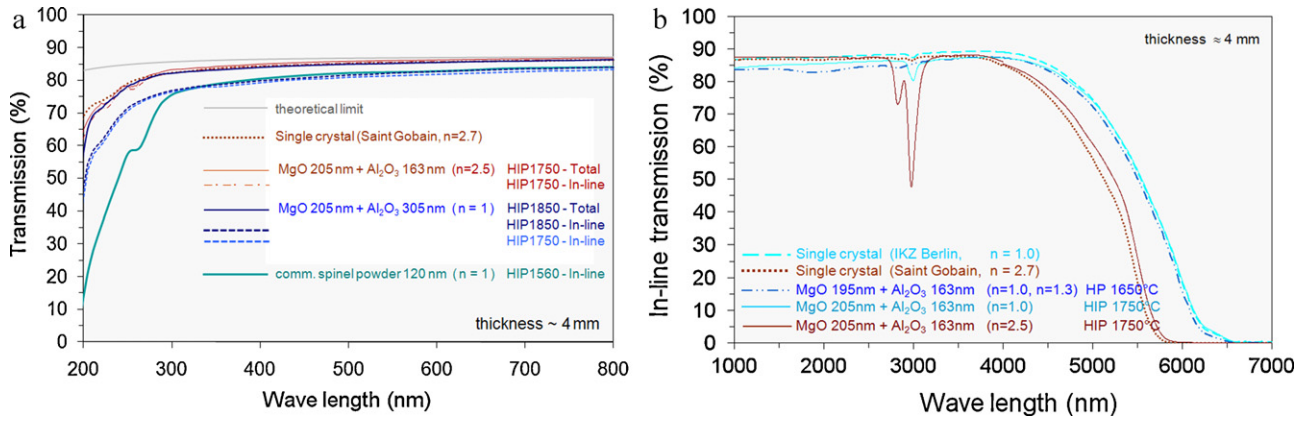

Fig. 7. (a) Transmission of bodies manufactured by pressing, pressure-less pre-sintering and HIP (i) from different MgO/Al_2O_3 mixtures, and (ii) from a 120 nm spinel powder (the UV transmission drops even more when still finer spinel powders are used[14]). The best results are compared with the spectrum of a spinel single crystal of similar composition. The upper line gives the theoretical limit ($=2n/(n^2+1)$, with n – refractive index [depending on the wave length]). (b) IR transmission of reactively sintered spinel starting from similar MgO and same α-Al_2O_3 as used for one of the samples in (a).

average Al_2O_3 particle size of 305 nm the spectrum is depressed to a lower level by incomplete sintering: a population of pores that cover a wide range of sizes is indicated now by the large difference between total and in-line curves.

This latter statement needs the comment that within the frame of the present study experiments with different compositions and starting with identical raw MgO/Al_2O_3 powders did *not generally* confirm the strong difference of the in-line spectra displayed in Fig. 7a for the reactively sintered ceramics with $n = 1$ and $n = 2.5$. Thus, the difference of these spectra in Fig. 7a has to be attributed primarily to the very coarse corundum powder (305 nm, 4.9 m^2/g) used for this individual test with $n = 1$ and not to some – speculative – impact of the composition on the final pore elimination during high-temperature HIP (note that Fig. 4c describes an influence of the composition during an earlier stage of sintering only – without a valid information about an eventual impact of Al-rich compositions on the final HIP densification).

The IR limit of the transmission in Fig. 7b is clearly dominated by a negative influence of Al-rich compositions. The general character of the recorded spectra[5] is as expected for spinel with, however, one remarkable detail: after optimized reactive processing the transparent windows do not exhibit the well-known for spinel absorption at ~2825 and 2980 nm commonly attributed to the incorporation of hydrogen into the spinel lattice (giving rise to OH stretching vibrations).[31–33] With Fig. 7b this problem can be minimized by right thermal processing: whereas in agreement with the literature[32] this absorption is *not generally* removed when alumina-rich spinel is replaced by $MgO{\cdot}1.0Al_2O_3$, alumina-*rich* spinel materials can, on the other hand, be manufactured e.g. with $n = 2.7$ *without* significant absorption in this range.

4. Discussion

The fundamentally different sintering performance of two differently synthesized spinel powders with similar average *particle sizes* and specific surfaces, similar narrow *pore size* distributions of the green bodies and with identical calcination and milling conditions is a major result of this investigation (Fig. 2b). The constancy of all parameters of calcination and processing, of nominally equal compositions, same particle sizes and homogeneity suggests that the different lattice structures indicated by the NMR spectra of Fig. 2c have significantly contributed to the different sintering temperatures. The real mechanism how the different cation disorder displayed by Fig. 2c contributes to the observed different sintering behavior cannot be explained here but it is commonly accepted that antisite defects govern the whole defect chemistry of magnesium aluminate.[26] Therefore, it is expected that these differences in the structures of the two spinel lattices will strongly influence the diffusion processes.

When such differences in structures of differently synthesized spinel lattices represent a third major factor that governs the sintering densification together with the particle size and the homogeneity of the green bodies, then it is highly probable that special lattice structures can have contributed to the exceptional transmittance results reported by Ikesue[12] (starting with a raw powder with 90% "spinelization") or achieved by reactive hot pressing by Tanaka et al.[13] In the present experiments this positive influence was confirmed by the improved reactive sintering of MgO/Al_2O_3 composite bodies (Fig. 3a) and, finally, by the increased in-line transmission of such bodies which coincides with the total transmittance and fits the spectrum of a single crystal of similar composition (Fig. 7a).

Comparing the sintering and NMR results of powders and of transparent compacts with 1:1 stoichiometry in Fig. 2b and c and in Fig. 4a it was concluded above that the temperatures of pre-sintering and HIP (>1500 °C in the present investigations) diminish the cation disorder. This conclusion agrees with a similar observation made by Morey et al. after annealing at 1450 °C.[20] In some contrast, several studies reported an *increase* of the Al–Mg inversion (measured by electron spin resonance or by NMR) of natural spinel minerals during annealing at moderate temperatures of 750–1400 °C[22,25] starting, however, from an extremely low inversion <5% as it appears typical for natural crystals with their very special growing conditions[24] and ending then at similar values as found for synthetic crystals of 1:1 stoichiometry. Interestingly, the direct high-temperature NMR

Please cite this article in press as: Krell A, et al. Influence of the structure of $MgO{\cdot}nAl_2O_3$ spinel lattices on transparent ceramics processing and properties. *J. Eur. Ceram. Soc.* (2012), doi:10.1016/j.jeurceramsoc.2012.02.054

measurements performed by Maekawa et al. also give some indication of a slightly *decreasing* inversion at temperatures >1350 °C.[22]

As to the relationship of antisite defects and sintering densification at different compositions in the range between $n = 1$ and $n = 1.5$ it has to be noted that a detail in Figs. 2b and c and 4a and c is only apparently in a conflict when similarly increasing cation disorder initiates *opposite* sintering effects: increasing antisite defects at higher alumina contents (Fig. 4a) *increase* the sintering temperatures of reactively formed spinel up to $n \sim 1.5$ (Fig. 4c) whereas they *reduce* the sintering temperatures of spinel powders with 1:1 stoichiometry (Fig. 2b and c). However, these observations refer to very different compositions and have, therefore, to be addressed differently: as outlined above it is the Mg deficit which in lattices with higher n values stimulates site exchange processes additionally to the smaller effects observed for different lattice structures with $n = 1$. Therefore, in spinel lattices with a 1:1 stoichiometry and in Al-enriched spinel changes in the cation disorder occur in different crystallographic environments and will imply different consequences for other defects and diffusion processes. The more recent literature expects that

- antisite defects in $MgAl_2O_4$ (i.e. at $n = 1$) should be associated with trimer Schottky defect clusters which include oxygen vacancies[18] (and should, therefore, *promote* diffusion and sintering as in Fig. 2b and c) whereas
- with *compositional* deviations cation exchange is expected to give rise to oxygen vacancies for Mg-rich compositions (with $n < 1$) only.[26]

The consequence is that moderate $n > 1$ should be accompanied by *retarded* sintering as in the left part of Fig. 4c and observed by an earlier study.[11]

The results of the phase analyses above have shown that the decrease of sintering temperatures observed in Fig. 4c for starting compositions with $n > 1.5$ must not be correlated with Al-rich spinel lattices because, surprisingly, no Al-rich spinel is formed on reactive pre-sintering of such MgO/Al_2O_3 mixtures. These observations need a more detailed explanation. A transformation of molar into volume amounts shows that for $n = 1.5$–2.0 the volume content of residual Al_2O_3 (associated with the formation of 1:1 spinel only) increases from 24 to 56 vol% with two consequences which both *promote* the sintering densification:

1. At high Al_2O_3 starting concentrations increased diffusion distances around the MgO particles require a longer time for solid state diffusion up to the equilibrium spinel composition than it is, apparently, available during 2 h of isothermal pre-sintering. Probably, this is the *kinetic* reason (not evident from phase diagrams) why starting from MgO/Al_2O_3 compositions with $n \geq 2$ spinel is formed with low $n \sim 1.0$–1.1. As outlined above, such 1:1 spinel sinters at lower temperature than reactively formed spinel lattices with $n = 1.2$–1.5.
2. Additionally, at $n > 1.5$ the continuous network of the excess alumina will promote the sintering densification since the alumina component typically exhibits a higher sintering activity than the spinel. This benefit will be active until the residual alumina is consumed at higher temperatures.

Since both processes depend on the increasing distance between the original MgO particles in alumina-rich MgO/Al_2O_3 mixtures (where MgO/Al_2O_3 interfaces are the nuclei of first spinel formation), the details of the sintering curve in Fig. 4c will depend e.g. on the particle size ratio of MgO and Al_2O_3 raw powders, and the shape of this curve will be different when starting e.g. with a mixture of $MgAl_2O_4$ and Al_2O_3 instead of using MgO. In fact, such experiments with $MgAl_2O_4$+Al_2O_3 showed a similar general shape of the curve of sintering temperatures as given by Fig. 4c but with smaller changes of the temperatures and with a maximum at lower n.

The best UV–vis transmission was achieved by reactive sintering of MgO/Al_2O_3 composites with starting particles of 150–200 nm and with a composition of $n = 2.5$ (Fig. 7a). However, *no* benefit of the alumina-rich composition was observed in the spectra of the *single crystals* in Fig. 6. Therefore, the *better* transmission of the reactively sintered spinel ceramic with $n = 2.5$ compared with the $n = 1$ composition in Fig. 7a has to be attributed to improved sintering and *not* to a higher *inherent* transmittance of the alumina-rich lattice.

In contrast to the UV to VIS and near-IR parts of the spectrum the IR-limit of the transmittance is clearly deteriorated by Al-rich spinel compositions (Fig. 7b). The absorption at about 3 μm wave length (commonly attributed to hydrogen in the spinel lattice[31–33]) has to be addressed differently: it is promoted by Al-rich compositions *only if* special chemical and thermal processing conditions enable the formation of this absorption band (Fig. 7b). Therefore, right thermal processing can provide Al-*rich* single crystals and sintered polycrystalline spinel ceramics *without* this absorption.

5. Conclusions

Extended investigations with $MgO{\cdot}nAl_2O_3$ single crystals which cover compositions between $n = 1$ and $n \sim 3$ did not reveal an impact of the stoichiometry on the inherent UV and visible transmissions (Fig. 6). The IR limit is, however, clearly deteriorated by higher n values (i.e. Al-rich compositions – Fig. 7b). On the contrary, the absorption at about 3 μm wave length *may be* intensified by a higher Al content but can be undetectably small even with $n \sim 3$ (Fig. 7b) and appears, therefore, dominated by *manufacturing* conditions.

Depending on the synthesis of spinel the cation disorder can differ significantly at 1:1 stoichiometry (Fig. 2c) and is, then, a third major influence on the sintering densification (Fig. 2b) together with particle size and homogeneity. This observation is the more important since several other complex transparent ceramics are commonly manufactured by reactive sintering of their components without a wider range of stoichiometric homogeneity. Nevertheless, some of these materials show indications that scattering losses associated with small compositional changes are caused not only by precipitates but also by changes of the lattice structures: recent reports observed a change of the *lattice* parameter in non-stoichiometric

Please cite this article in press as: Krell A, et al. Influence of the structure of $MgO{\cdot}nAl_2O_3$ spinel lattices on transparent ceramics processing and properties. *J. Eur. Ceram. Soc.* (2012), doi:10.1016/j.jeurceramsoc.2012.02.054

yttria-alumina garnet ($Y_3Al_5O_{12}$, YAG) although this material is always expressed as a line compound in phase diagrams.[34,35] It was, however, shown by ^{27}Al MAS NMR that the Al species in this garnet also occupy both octahedral AlO_6 and tetrahedral AlO_4 sites.[36] It is, therefore, expected that similarly strong effects as displayed by Fig. 2b for the sintering of different "stoichiometric" spinel lattices may also apply for other complex ceramics.

Sintering and HIP decrease the concentration of antisite defects compared with calcined spinel *powders* (Figs. 2c–4a). Despite this diminishing effect, HIP-ed bodies with different *compositions* ($n = 1$–2.5) exhibit *big* differences in their NMR spectra (Fig. 4a). This increase of antisite defects in alumina-rich spinel is accompanied by a decreasing lattice parameter (Fig. 4b) and *retards* the densification on reactive sintering as far as moderately Al-rich starting compositions are transformed into a single phase spinel ceramic of same composition. On the contrary, starting compositions with $n > 1.5$ increase the distance between the MgO particles in way that on pre-sintering a first spinel is formed close to a 1:1 stoichiometry, and these stoichiometric spinel particles are surrounded by a continuous network of corundum. These two effects *promote* the sintering and reduce the temperatures for the closure of pores (Fig. 4c).

By use of such means last pores were eliminated more readily by pressure-assisted *reactive* sintering of MgO/Al_2O_3 composites starting with *coarser* powders with median particle sizes of 100–200 nm instead of sintering pre-calcined raw spinel powders $\leq$100 nm. *Un*doped spinel ceramics were provided with an in-line transmittance which matches the spectra of single crystals with comparable composition from 200 nm wave length up to the IR range when the processing was fitted to the different needs of optimum UV, visible, and IR transmittance (Figs. 7a and b).

Acknowledgement

The authors gratefully acknowledge Dr. Erica Brendler from the Technical University Bergakademie Freiberg (Germany) who performed the NMR analyses.

References

1. Krell A, Blank P. The influence of shaping method on the grain size dependence of strength in dense submicrometre alumina. *J Eur Ceram Soc* 1996;**16**:1199–200.
2. Krell A, Klimke J, Hutzler T. Advanced spinel and sub-μm Al_2O_3 for transparent armour applications. *J Eur Ceram Soc* 2009;**29**:275–81.
3. Krell A, Klimke J. Effect of the homogeneity of particle coordination on solid state sintering of transparent alumina. *J Am Ceram Soc* 2006;**89**:1985–92.
4. Krell A, Hutzler T, Klimke J. Transmission physics and consequences for materials selection, manufacturing, and applications. *J Eur Ceram Soc* 2009;**29**:207–21.
5. Krell A, Waetzig K, Klimke J. Effects and elimination of nanoporosity in transparent sintered spinel. In: Tustison RW, editor. *Proceedings of SPIE: defense, security + sensing-window and dome technologies and materials XII, vol. 8016*. 2011. p. 801602, 1–10.
6. Reddy KPR, Cooper AR. Oxygen diffusion in magnesium aluminate spinel. *J Am Ceram Soc* 1981;**64**:368–71.
7. Bratton RJ. Initial sintering kinetics of $MgAl_2O_4$. *J Am Ceram Soc* 1969;**52**:417–9.
8. Oda I, Kaneno M, Hayakawa I. *Polycrystalline transparent spinel sintered body and method for producing the same*. Patent US – 4,273,587 (16.06.1981).
9. Sasame A, Shibata K-I, Fuji A, Nakayama S. *Spinel sintered body, light transmission window and light transmission lens*. Int. Patent Appl. WO – 2006/106670 A1 (12.10.06).
10. Dericioglu AF, Boccaccini AR, Dlouhy I, Kagawa Y. Effect of chemical composition on the optical properties and fracture toughness of transparent magnesium aluminate spinel ceramics. *Mater Trans* 2005;**46**:996–1003.
11. Ting C-J, Lu H-Y. Deterioration in the final-stage sintering of magnesium aluminate spinel. *J Am Ceram Soc* 2000;**83**:1592–8.
12. Ikesue A. *Transparent spinel ceramics, method for production thereof, and optical material using the transparent spinel ceramics*. Int. Patent Appl. WO – 2008/090909 A1 (23.01.08).
13. Tanaka M, Takahashi T, Hatamoto S. *Spinel sintered material*. Int. Patent Appl. WO – 2009/128269 A1 (16.04.09).
14. Krell A, Hutzler T, Klimke J, Potthoff A. Fine-grained transparent spinel windows by the processing of different nanopowders. *J Am Ceram Soc* 2010;**93**:2656–66.
15. Waetzig K, Krell A, Klimke J. *Verfahren zur Herstellung von redispergierbaren hochreinen Nanospinellpulvern, redispergierbares hochreines Nanospinellpulver und daraus erzeugte dichtgesinterte transparente Spinellprodukte [Process for the manufacture of redispersible high-purity spinel nanopowders and sintered transparent spinel components made thereof]*. German Patent Application DE – 10 2009 046 036 A1 (16.06.11).
16. Burnett JH, Kaplan SG, Shirley EL, Tompkins PJ, Webb JE. High-index materials for 193 nm immersion lithography. In: Smith BW, editor. *Proceedings of SPIE: optical microlithography XVIII, vol. 5754*. Washington: International Society for Optical Engineering; 2005. p. 611–21.
17. Burnett JH, Kaplan SG, Shirley EL, Horowitz D, Clauss W, Grenville A, et al. High-index materials for 193 nm immersion lithography. In: 2nd international symposium on immersion lithography. Bruges, Belgium, September 15, 2005.
18. Ball JA, Murphy ST, Grimes RW, Baconrisen RW, Smith R, Uberuaga BP, et al. Defect processes in $MgAl_2O_4$ spinel. *Solid State Sci* 2008;**6**:717–24.
19. Šepelak V, Indris S, Heitjans P, Becker KD. Direct determination of the cation disorder in nanoscale spinels by NMR, XPS, and Mössbauer spectroscopy. *J Alloys Compd* 2007, 434-5: 776-8.
20. Morey O, Goeuriot P. MgAlON spinel structure: a new crystallographic model of solid solution as suggested by ^{27}Al solid state NMR. *J Eur Ceram Soc* 2005;**25**:501–7.
21. Rigopoulos N, O'Donnell RG, Oh A, Trigg MB. An investigation of the solid solubility between aluminium oxynitride and magnesium aluminate spinels. *J Aust Ceram Soc* 2009;**45**:35–8.
22. Maekawa H, Kato S, Kawamura K, Yokokawa T. Cation mixing in natural $MgAl_2O_4$ spinel: a high-temperature ^{27}Al NMR study. *Am Mineral* 1997;**82**:1125–32.
23. Behrens H-J, Schnabel B. The second order influence of the nuclear quadrupole interaction on the central line in the NMR of quadrupolar nuclei using rapid sample spinning. *Physica* 1982;**114B**:185–90.
24. Smith ME. Application of ^{27}Al NMR Techniques to structure determination in solids. *Appl Magn Reson* 1993;**1/2**:1–64.
25. Schmocker U, Waldner F. The inversion parameter with respect to the space group of $MgAI_2O_4$ spinels. *J Phys C: Solid State Phys* 1976;**9**:L235–7.
26. Murphy ST, Gilbert CA, Smith R, Mitchell TE, Grimes RW. Non-stoichiometry in $MgAl_2O_4$ spinel. *Philos Magn* 2010;**90**:1297–305.
27. Okuyama Y, Kurita N, Fukatsu N. Defect structure of alumina-rich nonstoichiometric magnesium aluminate spinel. *Solid State Ionics* 2006;**177**:59–64.
28. Roy DM, Roy R, Osborn EF. The system $MgO–Al_2O_3–H_2O$ and influence of carbonate and nitrate ions on the phase equilibria. *Am J Sci* 1953;**251**:337–61.
29. Shukla P, Chernatynskiy A, Nino JC, Sinnott SB, Phillpot SR. Effect of inversion on thermoelastic and thermal transport properties of $MgAl_2O_4$ spinel by atomistic simulation. *J Mater Sci* 2011;**46**:55–62.
30. Krell A, Klimke J, Hutzler T. Transparent compact ceramics: inherent physical issues. *Opt Mater* 2009;**31**:1144–50.

Please cite this article in press as: Krell A, et al. Influence of the structure of $MgO{\cdot}nAl_2O_3$ spinel lattices on transparent ceramics processing and properties. *J. Eur. Ceram. Soc.* (2012), doi:10.1016/j.jeurceramsoc.2012.02.054

31. Wickersheim KA, Lefever RA. Optical properties of synthetic spinel. *J Opt Soc Am* 1960;**50**:831–2.
32. Fukatsu N, Kurita N, Shiga H, Murai Y, Ohashi T. Incorporation of hydrogen into magnesium aluminate spinel. *Solid State Ionics* 2002;**15**:2–153, 809-17.
33. Lenaz D, Skogby H, Nestola F, Princivalle F. OH incorporation in nearly pure $MgAl_2O_4$ natural and synthetic spinels. *Geochim Cosmochim Acta* 2008;**72**:475–9.
34. Patel AP, Levy MR, Grimes RW, Gaume RM, Feigelson RS, McCllellan KJ, et al. Mechanisms of nonstoichiometry in $Y_3Al_5O_{12}$. *Appl Phys Lett* 2008;**93**, 191902/1–3.
35. Gaume R, He Y, Markosyan A, Byer RL. Characterization of optical losses in transparent YAG ceramics. In: *6th laser ceramic symposium*. 2010.
36. Massiot D, Bessada C, Coutures JP, Taulelle F. A quantitative study of ^{27}Al MAS NMR in crystalline YAG. *J Magn Res* 1990;**90**:231–42.

Please cite this article in press as: Krell A, et al. Influence of the structure of $MgO{\cdot}nAl_2O_3$ spinel lattices on transparent ceramics processing and properties. *J. Eur. Ceram. Soc.* (2012), doi:10.1016/j.jeurceramsoc.2012.02.054